

Simulation of gaseous diffusion in partially saturated porous media under variable gravity with lattice Boltzmann methods

Jessica Furrer Chau and Dani Or

Department of Civil and Environmental Engineering, University of Connecticut, Storrs, Connecticut, USA

Michael C. Sukop

Department of Earth Sciences, Florida International University, Miami, Florida, USA

Received 17 November 2004; revised 24 March 2005; accepted 28 April 2005; published 12 August 2005.

[1] Liquid distributions in unsaturated porous media under different gravitational accelerations and corresponding macroscopic gaseous diffusion coefficients were investigated to enhance understanding of plant growth conditions in microgravity. We used a single-component, multiphase lattice Boltzmann code to simulate liquid configurations in two-dimensional porous media at varying water contents for different gravity conditions and measured gas diffusion through the media using a multicomponent lattice Boltzmann code. The relative diffusion coefficients (D_{rel}) for simulations with and without gravity as functions of air-filled porosity were in good agreement with measured data and established models. We found significant differences in liquid configuration in porous media, leading to reductions in D_{rel} of up to 25% under zero gravity. The study highlights potential applications of the lattice Boltzmann method for rapid and cost-effective evaluation of alternative plant growth media designs under variable gravity.

Citation: Chau, J. F., D. Or, and M. C. Sukop (2005), Simulation of gaseous diffusion in partially saturated porous media under variable gravity with lattice Boltzmann methods, *Water Resour. Res.*, 41, W08410, doi:10.1029/2004WR003821.

1. Introduction

[2] Plants growing under reduced gravity conditions play an important role in advanced life support systems for NASA's long-duration space exploration missions. Limited success in past plant growth experiments aboard various spaceborne platforms have been attributed to (among other factors) inadequate water and air management in plant growth media [Steinberg *et al.*, 2003]. Ongoing efforts focus on selection and characterization of porous media that support adequate fluxes of water, gases, and nutrients to plant roots and provide resilient growth conditions. Limited information regarding gaseous and liquid transport properties of porous media under variable gravity conditions hampers progress in selection and design of effective plant growth systems. Our primary objective is to develop and test methods that could fill in some of the knowledge gaps by focusing on fluid transport in granular media, specifically gas diffusion as affected by liquid configurations under microgravity.

[3] Oxygen is required for adequate plant root respiration, and is typically supplied through a partially saturated porous medium via gaseous pathways connected to the atmosphere. Liquid amounts and configuration in partially saturated porous media play a critical role in availability and continuity of these pathways, as gaseous diffusion through the liquid phase is about 10^4 times slower than through gaseous phase. Differences in liquid configuration between terres-

trial and reduced gravity conditions may impact the effective gaseous diffusion coefficient of plant growth media, thereby impacting oxygen supply to plant roots. Criteria for fluid management in plant root zones are often based on bulk variables (e.g., matric potential, water content) that may fail to reflect subtle differences in liquid configuration and could potentially lead to oversaturation and anoxic conditions in plant root zones.

[4] Recent studies have focused on the effect of microgravity on porous media bulk water retention properties. Jones and Or [1999] used a numerical model to solve the Richards equation for microgravity by removing the gravitational term in the equation and matched experimental data from Mir and a U.S. space shuttle. Their analysis of porous media parameters (soil water characteristic curve and hydraulic conductivity) on Earth and in microgravity suggested the presence of a narrower open pore size distribution in microgravity and limited participation of larger pores in water retention. The authors attributed these apparent changes to enhanced air entrapment and to particle rearrangement associated with acceleration and vibrations during liftoff.

[5] Parallel experiments have been conducted on Earth and in microgravity to quantify the effect of gravity on capillary wetting. Experiments aboard the Mir space station by Podolsky and Mashinsky [1994] revealed significant differences between one-dimensional capillary imbibition rates in microgravity and Earth's gravity, including higher water retention near the liquid reservoir under microgravity. In other experiments, Yendler *et al.* [1996] studied capillary imbibition through a pack of glass beads under true micro-

gravity conditions (aboard the Mir space station) and simulated microgravity conditions (horizontal capillary beds designed to reduce gravitational effects on Earth). They found that liquid front propagation in microgravity was slower than on Earth.

[6] *Schramm et al.* [2003] monitored capillary rise in bead pack cells under variable gravity conditions on a high-altitude parabolic flight profile airplane (European Space Agency Caravelle aircraft). For fluids that preferentially wet the glass beads (but not the Plexiglas walls of the cells), the authors obtained good agreement between experimental results and a finite difference model incorporating variable gravitational acceleration. They also ran a series of capillary flow experiments in sand pack cells aboard the NASA Discovery mission STS-91, finding imbibition rates for oil in sand to be somewhat higher (and much less stable) for microgravity than for Earth's gravity.

[7] The complexity and costs associated with conducting definitive experiments in space limit the scope and generality of conclusions that can be drawn from these studies. In *Schramm et al.*'s [2003] experiments, for example, vibrations during liftoff may have caused discontinuities in the sand pack. Additionally, automation constraints complicate accurate and meaningful data acquisition [*Keshock et al.*, 1998]. These and other limitations motivated our interest in developing alternative methods for simulating the impact of variable-gravity environments on transport processes in porous media as intermediate steps toward quantitative assessment and design. In this study, we employ a numerical method that could assist with design and prescreening of expensive space experiments rapidly, definitively, and cost-effectively.

[8] Our primary objective was to investigate the effects of variable gravity on liquid configuration and consequently on gaseous diffusion in partially saturated porous media. Since the macroscopic diffusive flux of gas is critically dependent on the water content and configuration, we first characterized the differences in liquid distribution under a gravitational acceleration ($1g$) and under $g = 0$ ($0g$ or microgravity). Simulations were performed first in a highly simplified two-dimensional porous medium, and then in a more realistic (but still 2-D) domain. The lattice Boltzmann method (LBM) was used to simulate liquid equilibration and distribution within these idealized porous media, and subsequently to simulate gas diffusion through the media at varying water contents. A gravitational force term was included in some simulations and not in others to allow comparison under different gravity conditions.

[9] LBM is a descendent of cellular automata, and it has been shown to preserve the physics of macroscopic fluid behavior based on simplified particle dynamics [*Nourgaliev et al.*, 2003; *Chen et al.*, 1996]. Another useful feature of the method is the ability to incorporate or remove effects of body forces (such as gravity) on the particles. By setting a single parameter equal to zero, the gravity can be turned off to allow for the simulation of fluids under $0g$.

[10] Macroscopic gas diffusion coefficients for partially saturated porous media are also obtained using a lattice Boltzmann code. The lattice Boltzmann method and its

ability to simulate gaseous diffusion will be described in greater detail in section 2.

2. Theoretical Background

[11] In sections 2.1 and 2.2, the theory of liquid configuration and gaseous diffusion in porous media is discussed. Section 2.3 contains a brief introduction to the LBM, and sections 2.4 and 2.5 describe validation of the LBM for simulating diffusion.

2.1. Liquid Configurations in Porous Media

[12] Here we consider a finite domain simulating a container filled with a porous medium. On Earth, the equilibrium distribution of a liquid in such a domain is governed by interplay between capillary and gravitational forces; in the absence of gravity, capillary forces alone determine the liquid's distribution. Consequently, in zero gravity we expect liquid to be retained in the smallest pore spaces where capillary forces are strongest. Under Earth's gravity, liquid still preferentially inhabits the smallest pores, but it is also driven to the bottom of the container by gravitational acceleration.

[13] The competition between gravity and capillarity in a porous medium is quantified by the dimensionless Bond number, given by

$$Bo = \frac{\Delta\rho g a^2}{\sigma}, \quad (1)$$

where $\Delta\rho$ is the density difference between the two fluids (air and water in an unsaturated medium), g is the acceleration due to gravity, a is the average pore size, and σ is the surface tension. Bo , a function of both fluid and porous medium properties, is a useful parameter for relating imbibition simulations to real-world flow scenarios. A typical Bo for liquid infiltration into a coarse-grained porous medium on Earth would be on the order of 10^{-3} , with typical values for finer-grained media of $Bo \leq 10^{-5}$ [*Freidman*, 1999]. Gravity-induced fingering (in contrast to stable infiltration) can be expected at $Bo > 10^{-2}$ [*Prazak et al.*, 1992]. Under microgravity conditions (i.e., on the ISS), the gravitational acceleration is approximately 10^{-3} times the value on Earth, resulting in $Bo \approx 10^{-6}$ for the coarse-grained plant growth media in current use.

2.2. Gas Diffusion in Porous Media

[14] Gaseous diffusion results from molecular-level collisions due to thermal agitation and causes transport from zones of high concentration of molecules to low concentration. Strict binary diffusion, or diffusion of species A in species B (with assumed isotropy in the diffusion coefficient), is governed by the diffusion equation:

$$\frac{\partial C_A}{\partial t} = -D_{AB} \nabla^2 C_A, \quad (2)$$

where D_{AB} is the binary diffusion coefficient. This simplified form of mass transport equation involves several assumptions including no advection, constant density of the species mixture, and equimolar counterdiffusion [*Welty et al.*, 2001, p. 461].

[15] Quantification of gas diffusion in partially saturated porous media requires estimation of a macroscopic effective diffusion coefficient that varies with the porosity and degree of saturation (or air-filled porosity). Early efforts at describing diffusion in soils focused on determining an effective cross-sectional area through which diffusion takes place. These geometrical arguments led to several models of the form $D_{eff}/D_0 = a\epsilon^b$, where D_{eff} is the effective diffusion coefficient through the porous medium, D_0 is the intrinsic diffusion coefficient or diffusion coefficient through open air, ϵ is the air-filled porosity, and a and b are constants [Marshall, 1959; Millington, 1959; Millington and Quirk, 1961; Millington and Shearer, 1971]. The expression D_{eff}/D_0 represents the macroscopic diffusion coefficient through a porous medium at a given air-filled porosity scaled by the value in open air and is referred to as the relative diffusion coefficient or D_{rel} .

[16] Moldrup *et al.* [2000] reviewed several of these models, and suggested the inclusion of a “water-induced linear reduction” (WLR) of D_{rel} to account for the effect of increased water content on the relative diffusion coefficient. The WLR term is simply the ratio of air-filled porosity to total porosity. The authors modified and tested several similar models; the one that we use here is the so-called Penman-Millington-Quirk (PMQ) model:

$$D_{rel} = 0.66\Phi\left(\frac{\epsilon}{\Phi}\right)^{\frac{12-m}{3}}, \quad (3)$$

where ϵ is air-filled porosity, Φ is porosity, and m is a fitting parameter. Note that porosity is constant while air-filled porosity is a function of volumetric liquid content θ ($\epsilon = \Phi - \theta$). The authors give $m = 6$ as the best fitting parameter for the sieved, repacked soils that they tested.

[17] Recent studies by *Altevogt et al.* [2003a, 2003b] have expanded the traditional transport equations for gas in porous media to account for nonideal effects such as diffusive slip flow. Slip flow occurs when the tangential gas velocity at the gas-solid interface is finite and nonzero, and becomes important in flow situations where neither diffusion nor advection dominate. Presently, however, the inclusion of such effects into diffusion models remains a challenge, and its importance for porous media gas diffusion processes awaits conclusive experimental confirmation. Hence we do not consider these effects in this study.

[18] Motivated by gaseous diffusion in plant growth media, we consider only diffusive transport with a no-slip boundary condition and no pressure-driven advection of gases. We have also assumed stationary liquid configurations at the onset of gas diffusion and throughout the process, thereby neglecting any consideration of phase interference due to liquid movement. (See *Fouar et al.* [1993] and *Persoff and Pruess* [1995] for discussions of phase interference in pressure-driven flow.)

2.3. Lattice Boltzmann Method

[19] Basic principles of the lattice Boltzmann method (LBM) were reviewed by *Sukop and Or* [2003, 2004]. A two- or three-dimensional grid is defined, and each node is initialized with a particle distribution function $f_a(\mathbf{x}, t)$ which represents the probability of finding a particle with position

\mathbf{x} and velocity \mathbf{e}_a at time t . The particle distribution evolves at each time step according to the equation

$$f_a(\mathbf{x} + \mathbf{e}_a\Delta t, t + \Delta t) = f_a(\mathbf{x}, t) - [f_a(\mathbf{x}, t) - f_a^{eq}(\mathbf{x}, t)]/\tau, \quad (4)$$

$$a = 0, \dots, b$$

where f^{eq} is the equilibrium distribution toward which each distribution is relaxed, τ is a relaxation parameter, and b is the number of directions that a particle can move to reach an adjacent node. (In our square 2-D lattice, $b = 8$; $a = 0$ refers to rest particles.) This governing equation incorporates the commonly used Bhatnagar-Gross-Krook (BGK) approximation to the collision operator [Succi, 2001]. The density of particles $\rho(\mathbf{x}, t)$ and the macroscopic velocity $\mathbf{u}(\mathbf{x}, t)$ at each node are given by

$$\rho(\mathbf{x}, t) = m \sum_a f_a(\mathbf{x}, t) \text{ and } \mathbf{u}(\mathbf{x}, t) = \frac{m \sum_a f_a \mathbf{e}_a}{\rho(\mathbf{x}, t)}, \quad (5)$$

respectively, where m is the particle mass. The equilibrium distribution f^{eq} is given by

$$f_a^{eq}(\mathbf{x}) = w_a \rho(\mathbf{x}) \left[1 + 3 \frac{\mathbf{e}_a \cdot \mathbf{u}}{c^2} + \frac{9}{2} \frac{(\mathbf{e}_a \cdot \mathbf{u})^2}{c^4} - \frac{3}{2} \frac{u^2}{c^2} \right] \quad (6)$$

where c is the lattice constant $\Delta x/\Delta t$, $w_0 = 4/9$, $w_a = 1/9$ for $a = 1 \dots 4$, and $w_a = 1/36$ for $a = 5 \dots 8$.

[20] To incorporate forces acting on particles, the equilibrium distribution f^{eq} is computed with a modified velocity $\mathbf{u}'(\mathbf{x}, t)$ based on the addition of momentum terms at each time step as follows:

$$\rho(\mathbf{x}, t) \mathbf{u}'(\mathbf{x}, t) = \rho(\mathbf{x}, t) \mathbf{u}(\mathbf{x}, t) + \tau \frac{d\mathbf{p}}{dt}(\mathbf{x}, t) + \tau \mathbf{F}_{ex}(\mathbf{x}, t). \quad (7)$$

Here \mathbf{F}_{ex} is an external force such as gravity, while $\frac{d\mathbf{p}}{dt}$ is the change in momentum due to the attraction between particles at neighboring nodes and is given by

$$\frac{d\mathbf{p}}{dt} = -G\psi(\mathbf{x}, t) \sum_a \psi(\mathbf{x} + \mathbf{e}_a\Delta t, t) \mathbf{e}_a, \quad (8)$$

where G is an interaction strength parameter and $\psi(\mathbf{x}, t)$ is the potential at each node. Different forms of the ψ function can be employed to produce different equations of state for the simulated fluid. In our simulations, we used a nonideal equation of state which allows for phase changes in the fluid (condensation and evaporation). See *Sukop and Or* [2003, 2004] for a description of our code's development.

[21] The preceding description was for a single-component lattice Boltzmann code; that is, only one type of particle is released in the domain. With slight modifications, two or more fluids with different properties may coexist in the domain. This allows for the simulation of the behavior of two miscible or immiscible fluids in porous media, for example [Shan and Chen, 1994].

2.4. Modeling Diffusion Using the Lattice Boltzmann Method

[22] Several papers have been published on simulating diffusion with the LBM [Shan and Doolen, 1996; Yoshino

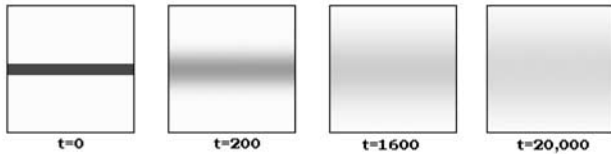


Figure 1. Simple LBM simulation of a strip of blue gas diffusing through white gas. Bounce-back boundary conditions are applied at the domain boundaries. See color version of this figure in the HTML.

and Inamuro, 2003; D'Souza et al., 2002; Merks et al., 2003; Flekkøy, 1993]. In order to simulate the diffusion of a gas in the air-filled fraction of a porous medium, we used a two-component LB code. In order to produce two miscible gases, the interaction parameter for particles of different types was set to zero; that is, the gas molecules neither attracted nor repelled each other. “Air” was visualized as white and “gas” (such as oxygen) was visualized as blue. The gases had identical properties; no attempt was made to distinguish them based on density variations or other considerations.

[23] Figure 1 shows a strip of blue “oxygen” diffusing through white “air.” There are solid boundaries on all sides of the domain, which produces a “bounce-back” boundary condition; that is, any gas particle that collides with the wall is reflected back into the domain. The images clearly show the diffusion of the gases proceeding from sharply delineated regions to uniform concentrations of both gases throughout the domain.

[24] The LBM diffusion model has an intrinsic diffusion coefficient D_0 that depends on the value of τ according to [Yoshino and Inamuro, 2003]

$$D_0 = \frac{1}{3} \left(\tau - \frac{1}{2} \right). \quad (9)$$

Hence the theoretical diffusion coefficient for the LBM using $\tau = 1$ is $D_0 = 1/6 \text{ lu}^2 \text{ ts}^{-1}$ (lattice units squared per time step).

[25] To verify that the diffusive behavior predicted by the LBM is quantitatively correct, we conducted several diffusion simulations in simple geometries and compared the results with analytical solutions of the diffusion equation.

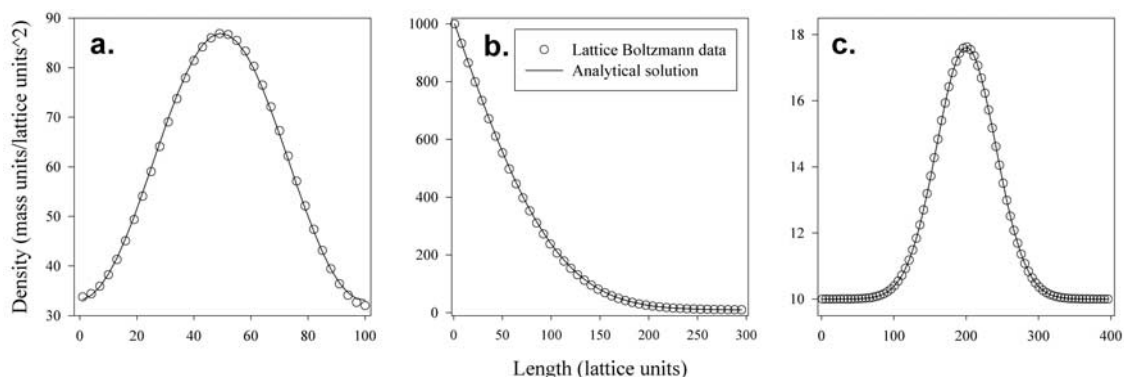


Figure 2. LBM diffusion data compared with analytical solutions: (a) 1-D instantaneous line source, (b) 1-D infinite source, and (c) 2-D instantaneous point source (x direction).

All simulations used strict binary gas diffusion; no solid or liquid phase was introduced. The results obtained by the LB code were in excellent agreement with analytical solutions (Figure 2).

2.5. Effective Diffusion Coefficient

[26] Having established that the LBM successfully simulates binary diffusion processes in the absence of solids, we proceed to compute an effective diffusion coefficient through a porous domain with known theoretical behavior. We considered Maxwell’s equation for diffusion through a dilute pack of spheres, employing a correction by Rayleigh for denser sphere packings [Crank, 1975; Bird et al., 2002, equation 9.6–2]. Maxwell’s equation is

$$\frac{D_{eff}}{D_0} = 1 + \frac{3v_1}{\left(\frac{D_1 + 2D_0}{D_1 - D_0} \right) - v_1 + C}, \quad (10a)$$

$$C = 1.569 \left(\frac{D_1 - D_0}{3D_1 - 4D_0} \right) v_1^{10} + \dots \quad (10b)$$

where component 0 is air (white) with $D_0 = 1/6 \text{ lu}^2 \text{ ts}^{-1}$ (from equation (9)), component 1 is solid with $D_1 = 0$, and C is a correction term applied only for dense volume fractions. Comparison of this model, written for diffusion through a pack of three-dimensional spheres, with our 2-D simulations, which effectively model diffusion through a pack of cylinders, requires a geometrical volume fraction correction ($V_{cylinder} = 3/2 V_{sphere}$).

[27] Diffusion through domains with varying volume fractions of solid spheres was simulated with the LBM, and the flux J through each system was calculated. We then employed Fick’s law ($J = D_{eff} dC/dx$) to obtain D_{eff} . The LBM diffusion results were in very good agreement with values predicted by the corrected Maxwell equation (within 4%, up to volume fractions of 0.55). We therefore concluded that the LBM adequately simulates gaseous diffusion through a simple porous domain.

3. LBM Numerical Experiments

[28] The lattice Boltzmann simulations were carried out in two steps. First the equilibrium liquid distribution was established in the porous medium using a single-component LBM code with a nonideal equation of state [Sukop and Or,

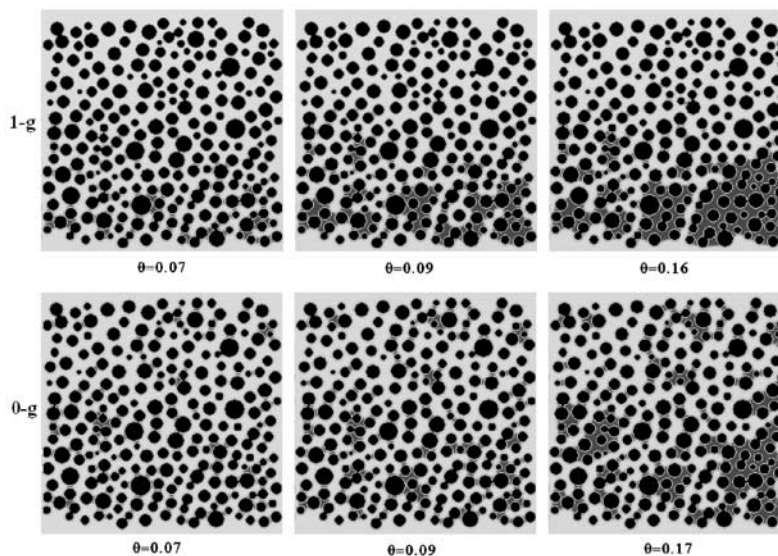


Figure 3. Liquid in its equilibrium position in an idealized porous medium. Differences between liquid configurations under 1g and 0g for similar water contents will result in different gaseous diffusion coefficients through each domain. See color version of this figure in the HTML.

2003, 2004]. Liquid distributions obtained in these simulations were used as the initial conditions for gas diffusion simulations.

3.1. Step One: Equilibrium Liquid Configurations

[29] Setting the density of the fluid at the boundaries, the fluid was allowed to enter the domain and attain its equilibrium distribution based on the geometry of the simulated porous medium. Setting the density at the boundaries of an LBM simulation is equivalent to prescribing the matric potential at the boundaries of the porous medium. Varying the density/matric potential allowed the fluid to occupy the domain at varying liquid contents. Two sets of simulations were produced: one set generated varying liquid contents under zero gravity, and the other did the same under gravity. Figure 3 shows images generated by the LB code of the fluid in its equilibrium position in the complex domain for three gravity/no-gravity pairs. (Dark blue is liquid, light blue is vapor, black is solid.)

[30] The results in Figure 3 illustrate the impact of gravity on the equilibrium arrangement of liquid in the pore space. In the absence of gravity the arrangement is entirely defined by capillary forces, and liquid preferentially invades the smallest pore spaces. The effect of gravity is to force the liquid to fill larger pores at the bottom of the domain that it would not otherwise occupy under the prescribed density/matric potential. This creates an increasingly saturated layer that will significantly impact gaseous diffusion through the domain because many pathways for vertical diffusion become blocked.

[31] Generally, we observed lower amounts of liquid in the domain under gravity than obtained under zero gravity for identical boundary conditions. This effect is due to enhanced liquid “drainage” under the influence of gravitational forces absent in the 0g case. The difference is not evident from Figure 3 because different boundary density values were used for 0g and 1g to obtain nearly identical equilibrium liquid contents.

3.2. Step Two: Simulation of Gaseous Diffusion

[32] In the second phase of our experiment we used the results from the equilibrium liquid distribution step (see Figure 4a) and converted each liquid node to a solid-like node, creating a new domain wherein both solids and liquids were impervious to gaseous diffusion (Figure 4b). That is, $D_{gas-liquid} = D_{gas-solid} = 0$ in our simulations. The justification for this approximation is the very low rate of gas diffusion through liquid relative to that through gas-filled pores (about 4 orders of magnitude difference). We then calculated gaseous diffusion through the new domain. Gaseous diffusion simulations were performed without an applied gravitational acceleration; only the liquid configuration simulations were performed under variable gravity.

[33] Gaseous diffusion experiments were run vertically and horizontally through the converted domains using periodic (wraparound) boundaries on the sides parallel to the diffusive flux and constant density (concentration) boundaries on the sides of the domain perpendicular to the diffusive flux. The effective diffusion coefficients across

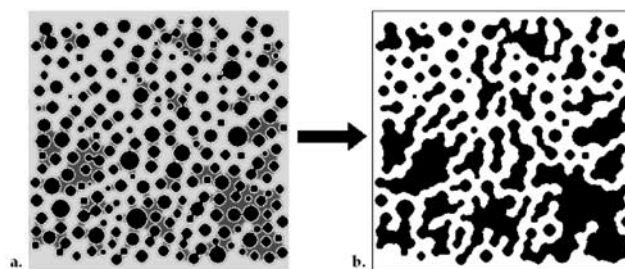


Figure 4. (a) Simulated liquid configuration in equilibrium position in the porous medium. (b) Liquid-filled nodes are converted to nondiffusive solid-like nodes for subsequent gaseous diffusion calculations. See color version of this figure in the HTML.

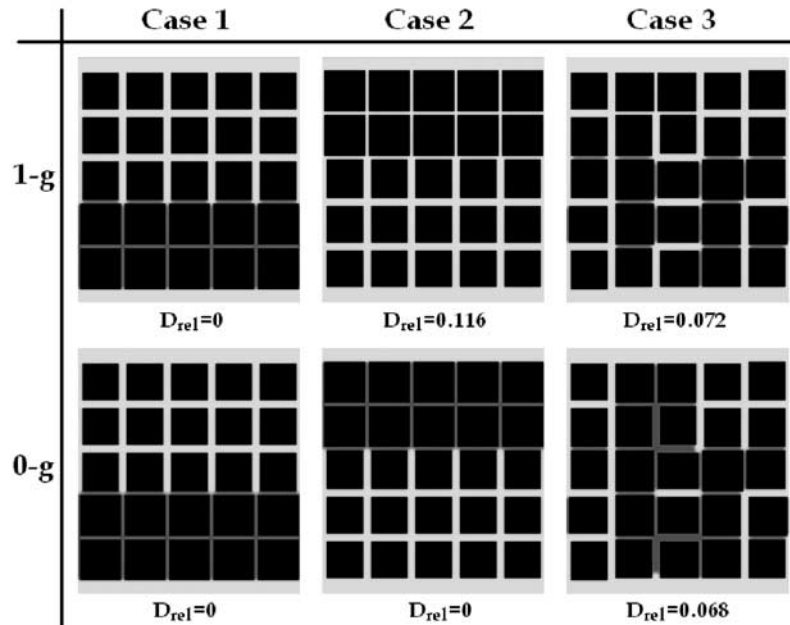


Figure 5. Simplified porous medium with (1) small pores at the bottom of the domain, (2) small pores at the top, and (3) small pores randomly distributed throughout. All plots show equilibrium positions of liquid and were generated under the same density boundary conditions (analogous to equal matric potentials). Diffusion coefficients were calculated in the vertical direction. See color version of this figure in the HTML.

the domain were calculated with a macroscopic application of Fick's law:

$$J = -D_{eff} \frac{\Delta C}{\Delta z}. \quad (11)$$

The equilibrium flux of gas through the domain was measured and divided by the concentration gradient across the system to obtain D_{eff} .

4. Results and Discussion

4.1. Gaseous Diffusion in a Simple Pore Network

[34] To illustrate the complex interplay between gravitational acceleration, porous medium structure and liquid configurations, we constructed a 2-D pore network with porosity $\phi = 0.31$. The rectangular “pores” separating square solid particles were either 3 or 7 pixels in width. This simple bimodal pore size distribution allows for prediction of the effect of gravity on liquid distribution. We tested three cases with similar pores distributed differently in the domain and subject to identical boundary conditions. Constant density/matric potential boundary conditions were used. Because of the relationship between pore size and potential, all the pores of the same size empty or fill at a critical potential value. The boundary conditions used in this series of simulations were such that under 0g (capillary forces only), the small pores (3 pixel width) would fill, but the large pores (7 pixel width) would remain empty. The additional influence of gravity produces some alteration in the liquid configuration and therefore in the effective diffusion coefficient.

[35] The three cases and corresponding equilibrium liquid distributions are illustrated in Figure 5. In case 1, placing small pores at the bottom of the domain creates a situation in which the liquid distribution is invariant under 0g and 1g; hence no difference in the effective gas diffusion coefficient is observed. In case 2, placing the small pores at the top of the domain results in different liquid configurations since the pores at the bottom of the domain are too large to retain the liquid driven into them by gravity. This different liquid configuration translates into a large difference in D_{eff} . Finally, in case 3 we distributed the pores randomly throughout the domain. Three realizations with randomly determined pore arrangements were created, and the resulting D_{eff} values were averaged. (Only one realization is shown in Figure 5.) Case 3 produces some difference in the liquid configuration and consequently in D_{eff} , but not as extensive as the difference observed in case 2.

[36] Figure 5 shows the equilibrium images generated by LBM simulations in the simplified domain. The “gravity” images for cases 1 and 2 clearly show the competing influences of gravity and capillarity; in case 1 they work together to hold liquid in the small pores at the bottom of the domain, while in case 2 the forces are opposed and no liquid is retained. In case 3 the effects of gravity are again clearly illustrated. Under gravity only the small pores in the bottom of the domain retain liquid, while under 0g all the small pores are filled, in addition to some large pores confined by small pores.

[37] The simulations shown in Figure 5 have volumetric (actually areal) liquid contents between $\theta = 0$ and $\theta = 0.06$. (For cases 1 and 2, $\theta = 0.05$ or 0. For the three realizations of case 3, $0.02 \leq \theta \leq 0.06$.) Effective diffusion coefficients for these domains were calculated in the vertical direction

Table 1. Relative Diffusion Coefficients for 1g and 0g Simulations

0g D_{rel}			1g D_{rel}		
Air-Filled Porosity	Horizontal	Vertical	Air-Filled Porosity	Horizontal	Vertical
0.6786	0.4419	0.4579	0.6786	0.4419	0.4518
0.6251	0.2675	0.2799	0.6318	0.3087	0.2582
0.6064	0.2367	0.2421	0.6112	0.2971	0.2250
0.5939	0.2229	0.2126	0.5867	0.2964	0.1933
0.5763	0.2211	0.2078	0.5428	0.2796	0.1734
0.5475	0.2103	0.2007	0.5058	0.2456	0.1248
0.5299	0.2024	0.1935	0.4285	0.1914	0.0664
0.5115	0.1964	0.1738			
0.4076	0.1520	0.0658			

using the multicomponent LB code and are reported on a relative basis.

[38] Because of the limited number of pore sizes, small changes in potential (controlled by boundary conditions) induce large changes in water content. All small pores empty or fill at some critical potential, whereas large pores remain open until the potential is very close to zero. This effectively limits attainable air-filled porosity to three values: $\varepsilon = 0$ (full saturation), $\varepsilon = 0.31$ (zero saturation), and intermediate determined by the geometry. Clearly the effects of gravity on water content and therefore on gaseous diffusion will be minimal at zero and full saturation, while the effects will be greatest at intermediate water contents. It is evident from the D_{rel} values in Figure 5 that the greatest difference in vertical diffusion occurs for case 2, while for case 3 the difference is observable but small.

[39] These results from a simple pore network highlight the importance of pore space layering and porous media packing on diffusion behavior in reduced gravity. By controlling the pore arrangement of engineered plant-growth materials, one can in effect control the liquid configuration in the medium and thereby determine the available pathways for gas diffusion under various water contents. This allows for design of materials which optimize the desired transport properties.

4.2. Gaseous Diffusion in a Partially Saturated Porous Medium

[40] Here we present simulations performed in a more realistic 2-D porous medium as an extension of case 3 above. Solid disks of varying diameters were randomly placed in a domain, creating a random distribution of pore sizes. The domain size was 300×300 lattice units (lu), with an average pore diameter of 5.4 lu. Liquid imbibition into this domain was performed under $Bo = 0$ and $Bo \approx 10^{-2}$. This value for the gravity simulations is within the Bo range for gravity-driven infiltration on Earth (see section 2.1).

[41] Results from this series of simulations are shown in Figure 4. Clearly this is a very simplified approximation of a real porous medium, and subject to error (e.g., finite size effects, lack of randomness). Nevertheless, the behavior of gaseous diffusion coefficients as a function of air-filled porosity compares quite well to both measured diffusion data and empirical models within the achievable range of air-filled porosity of the medium.

[42] Table 1 summarizes the relative diffusion coefficients for the 1g and 0g simulations as a function of air-filled porosity. Because of the limited number of pore spaces in the idealized medium, no values less than $\varepsilon \approx 0.4$ could be used to simulate gas diffusion. While no limit exists on the equilibrium liquid contents the model can generate, below $\varepsilon \approx 0.4$ all diffusion pathways were blocked with liquid, reducing D_{eff} to zero. This effect could of course be mitigated by using a larger domain; however, the increased computing resources required made this step unfeasible for us at present.

4.2.1. Comparison With Measured Diffusion Data and Parametric Models

[43] Jones *et al.* [2003] used thin and horizontally oriented diffusion cells to measure diffusion of O_2 with minimal gravitational effects through partially saturated granular media. Water contents inside the cells were prescribed using pressure control through a porous stainless steel plate in contact with the porous medium in the cell. The cells were purged with nitrogen, and oxygen concentrations were maintained constant at the inlet of the cell and monitored at the outlet. The results were fitted to an analytical model to determine the effective diffusion coefficient [Glauz and Rolston, 1989]. Their results, plotted in Figure 6 as relative diffusion coefficients versus relative air-filled porosity, show excellent agreement with our LBM simulations for gaseous diffusion through the idealized porous medium. The measured air-filled porosities were scaled by available porosity in the two porous media. Jones *et al.*'s [2003] macroporosity available for diffusion was 0.37 (total porosity $\phi = 0.74$) whereas the porosity of our simulation domain was $\phi = 0.68$. The deviations at the lower air-filled porosity values and the drop-off to zero below $\varepsilon \approx 0.4$ are attributable to finite size effects (limited number of diffusion pathways) in our 2-D simulations. Below a threshold ε value, no further pathways are available for gas diffusion. This phenomenon also occurs in real soils, but the critical ε value would be lower and the decrease much more gradual.

[44] The LBM simulation results were also fitted with several parametric models from the Moldrup *et al.* [2003] review. Our gravity simulation data showed excellent agreement with the Penman-Millington-Quirk model with "water-induced linear reduction" factor (equation (3)). The value of the fitting parameter m for the LBM gravity data was 5.0, compared to $m = 6$ for the soils tested by the authors, and the data was in near-perfect agreement with the model at zero saturation, where $\frac{\varepsilon}{\phi} = 1$. (See Figure 6.) Fitting the model to the 0g data resulted in $m = 0.8$. The parametric model was not able to produce a good match with the 0g results; this is not surprising given that it is empirical in nature and the data used for its development was gravity influenced.

4.2.2. Comparison of Diffusion Under 0g and Gravity

[45] Diffusion coefficients for all simulations are shown in Figure 7. We simulated diffusion in the horizontal direction (transverse to gravity) and in the vertical direction (along the direction of gravity). In the vertically oriented diffusion simulations, gas was forced to pass through a nearly saturated layer at the bottom of the domain, creating a situation in which the D_{eff} value for the whole simulation was controlled by one layer of the medium. This situation

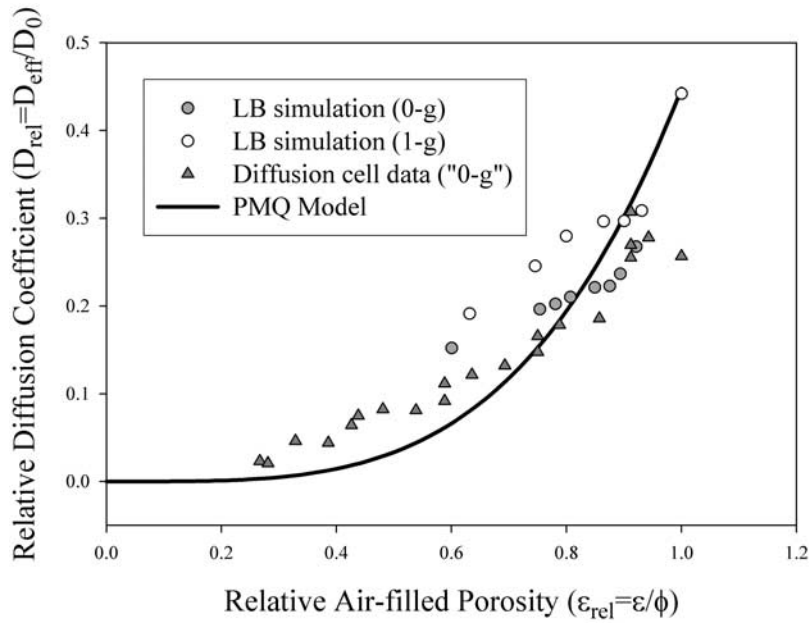


Figure 6. Simulated vertically oriented diffusion data plotted with actual gas diffusion cell data from Jones et al. [2003] and Moldrup et al.'s [2000] Penman-Millington-Quirk model.

does not necessarily reflect conditions affecting gaseous diffusion to plant roots, which may be located throughout the porous medium and not just in the saturated bottom layer. Therefore the horizontal simulations provide a more realistic characterization of the effect of gravity on diffusion in plant growth media, and only these results are considered in the following discussion.

[46] As expected, gaseous diffusion in the horizontal direction in 0g is lower than in 1g. This is attributable to the uniform liquid distribution under 0g affecting diffusion

at all depths equally. Under gravity, liquid draining from large pores accumulates at the lower part of the domain, thereby opening more pathways for horizontal gaseous diffusion at the top part of the domain than exist in the 0g case. The absence of these unblocked pathways under 0g is the cause of the observed reduction in D_{rel} . In our 2-D representation of a porous medium, gas diffusion was reduced by a maximum of 25%. The percent reduction in D_{rel} as a function of air-filled porosity is shown in Figure 7 (inset).

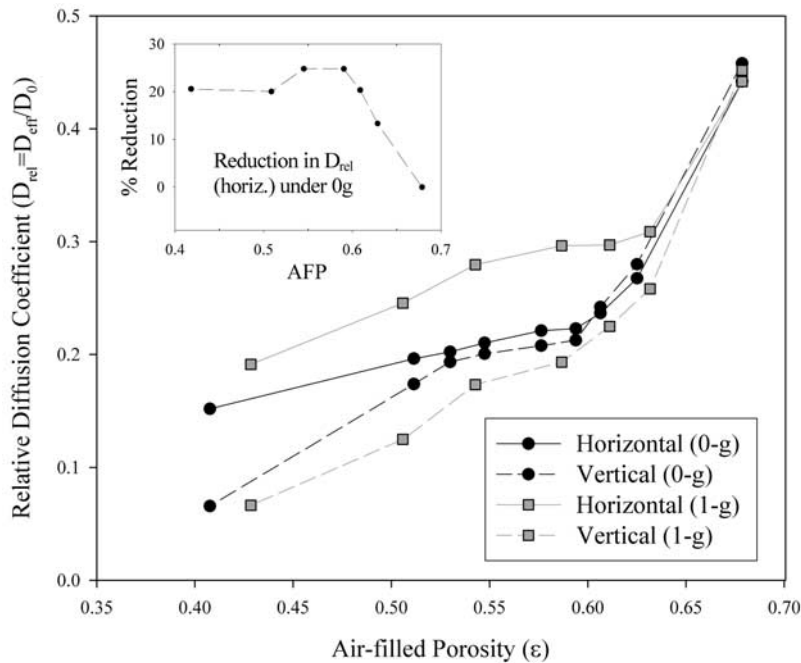


Figure 7. Relative diffusion coefficients for LB-simulated vertically and horizontally oriented diffusion. Inset shows percent reduction in horizontally oriented diffusion coefficient between 1g and 0g.

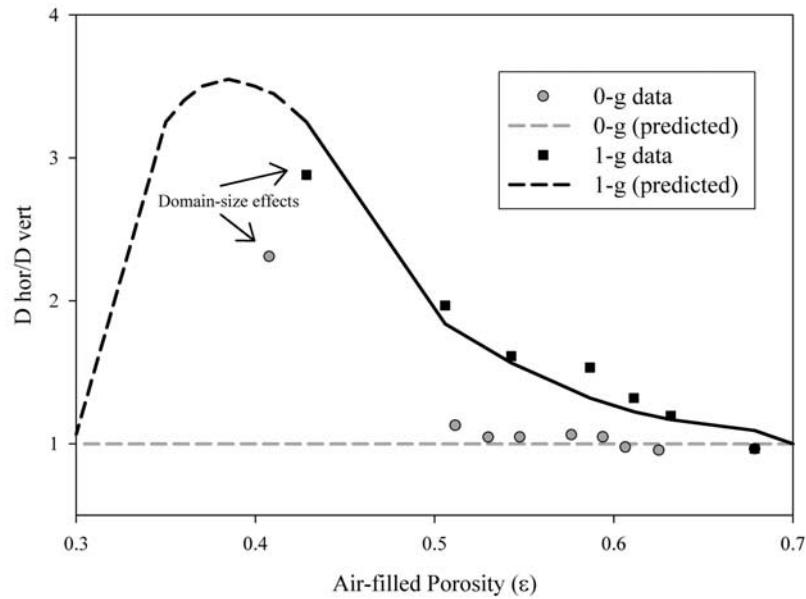


Figure 8. D_{hor}/D_{vert} for 0g and gravity simulations. Predicted plots follow *Jones et al.* [2003] and are qualitative in nature.

[47] These findings have potentially serious consequences for plant growth in microgravity. In growth media with randomly distributed pore sizes, water will be held primarily in the smallest pores by capillary forces, creating the discontinuous water phase observed in the LB simulation results. This evenly distributed liquid configuration reduces diffusive flux of gases to plant roots, depriving them of oxygen (and restricting removal of CO_2). The effects of gravity on liquid configuration, and therefore on gas diffusion, will be greatest at intermediate water contents and least at zero and full saturation.

[48] In contrast, simulated D_{eff} values for diffusion in the vertical direction for 1g were lower than D_{eff} for 0g, but only slightly. (See Table 1.) The difference is generally greatest at intermediate values of ϵ and tapers off at low and high ϵ , and is due to differences in liquid configuration under 0g and 1g. This result is consistent with our findings for the simple pore network with randomly arranged small and large pores.

[49] We formalize the effects of liquid stratification due to gravity on gaseous diffusion by comparing the horizontal and vertical diffusion coefficients for a given air-filled porosity. In 0g, we expect orientation to have little effect on the diffusion coefficient because the liquid is uniformly distributed throughout the domain (provided pore sizes are uniformly distributed). That is, in 0g we expect $D_{hor}/D_{vert} \approx 1$ for all air-filled porosities. Under 1g, we expect $D_{hor}/D_{vert} = 1$ at zero and full saturation (where there is no change in liquid configuration) and $D_{hor}/D_{vert} > 1$ at intermediate air-filled porosities (where the effect of the resistive bottom layer will be greatest for vertical diffusion and least for horizontal diffusion).

[50] Figure 8 depicts D_{hor}/D_{vert} for 0g and 1g simulations, showing a similar trend to that postulated by *Jones et al.* [2003] where the ratio is approximately equal to 1 for 0g and deviates (becomes >1) for intermediate saturation values under gravity. The high values of the ratio at low air-filled porosities for both 1g and 0g are due to domain-

size effects. The simulated “soil” represented by our 2-D domain contains a limited number of diffusion pathways. When a critical number of them are blocked by liquid, gaseous diffusion abruptly shuts down instead of decreasing gradually as expected in real soil, and D_{vert} becomes essentially zero. This will eventually happen for D_{hor} as well, but at a much lower air-filled porosity (beyond the achievable range of our simulations). Therefore D_{hor}/D_{vert} approaches infinity before D_{hor} finally drops to zero. In a real soil, we would expect a more gradual increase of D_{hor}/D_{vert} with increasing saturation until a point where D_{hor} becomes low enough to bring the ratio to one. In Figure 8 the predicted value of D_{hor} is based on the average air-filled porosity for the whole domain, while D_{vert} is determined by the air-filled porosity of the layer with highest water content. Predicted values are calculated using the PMQ model (equation (3)) fit to the LBM gravity data. The dashed portion of the predicted plot is a qualitative prediction based on the expected behavior of gas diffusion in the porous medium [*Jones et al.*, 2003].

5. Summary and Conclusions

[51] We presented results of lattice Boltzmann method (LBM) simulations of gaseous diffusion in partially saturated porous media under different gravity conditions. In the first step, we established the equilibrium distribution of liquid in media pore spaces considering two idealized porous media (a simple pore network and randomly distributed solid disks) under Bond numbers representative of Earth’s gravity and zero gravity. Subsequently, “freezing” the liquid distribution and assuming the diffusion coefficient of gas through liquid to be negligible, we measured the vertical and horizontal effective diffusion coefficients through the porous media at varying air-filled porosities.

[52] We found significant differences in liquid configurations between 1g and 0g. In the absence of gravity, liquid is held in the smallest pore spaces due to the dominance of

capillary forces; with gravity, liquid tends to accumulate at the bottom of the domain. Our simulations in a simple pore network demonstrated the effect of liquid distribution (layering) relative to the gravitational field on gaseous diffusion through the network. In a more complex domain, we simulated gas diffusion through a 2-D porous medium at varying air-filled porosities. For horizontal diffusion (representative of actual diffusive conditions around plant roots), 0g diffusion coefficients were lower than corresponding values under gravity due to a relatively uniform distribution of liquid under 0g. For vertically oriented diffusion, the formation of a layer with high saturation at the bottom of the domain resulted in artificially higher diffusion coefficients under 0g than under 1g. Plotting $D_{\text{hor}}/D_{\text{vert}}$ provides a measure of the effect of gravity (saturation stratification) on gaseous diffusion. Under 0g, $D_{\text{hor}}/D_{\text{vert}} \approx 1$ for all values of air-filled porosity because of the lack of gravity-induced liquid layers. Under 1g, $D_{\text{hor}}/D_{\text{vert}}$ is close to one for zero and complete saturation, and is maximal at some intermediate air-filled porosity.

[53] We conclude that gravity's effect on gaseous diffusion in porous media is highly dependent on the pore size distribution and pore arrangement in the medium relative to gravitational field (as these factors determine the liquid configuration), and also on water content. At very high and very low water contents, gas diffusion coefficients are similar under 0g and 1g; the greatest difference in liquid configuration and therefore in D_{eff} occurs at intermediate water contents.

[54] The dependence of gravitational effect on pore arrangement has important implications for plant growth media design for microgravity. Our two-dimensional representations of traditional porous media exhibit reduced gas diffusion by up to 25% under 0g due to differences in liquid configuration. This signals a need to expand research focus to engineered media in which gas diffusion pathways are prescribed (for example, by including water-repellant channels through the medium as gas conduits), thereby ensuring the adequate flux of gases to plant roots.

[55] Our study illustrates the potential usefulness of LBM as a tool to select and cost-effectively evaluate the performance of plant growth media designs under different gravitational and water supply scenarios. The lattice Boltzmann method accurately reproduces fluid dynamics under gravity and produces results consistent with theory for 0g. It is also capable of easily simulating fluid processes in complex domains, and even simple 2-D simulations can produce valuable insights into fluid transport in porous media. Therefore it offers a useful platform for the study of fluid behavior in microgravity.

[56] **Acknowledgments.** We gratefully acknowledge the support of NASA under grants 01-OBPR-01-009 and NAG 9-1284. We wish to thank Scott B. Jones (Utah State University) for access to diffusion cell measurements.

References

- Altevogt, A. S., D. E. Rolston, and S. Whitaker (2003a), New equations for binary gas transport in porous media, part 1: Equation development, *Adv. Water Resour.*, *26*, 695–715.
- Altevogt, A. S., D. E. Rolston, and S. Whitaker (2003b), New equations for binary gas transport in porous media, part 2: Experimental validation, *Adv. Water Resour.*, *26*, 717–723.
- Bird, R. B., W. E. Stewart, and E. N. Lightfoot (2002), *Transport Phenomena*, 2nd ed., John Wiley, Hoboken, N. J.
- Chen, S., D. Martinez, and R. Mei (1996), On boundary conditions in lattice Boltzmann methods, *Phys. Fluids*, *8*(9), 2527–2536.
- Crank, J. (1975), *The Mathematics of Diffusion*, 2nd ed., Clarendon, Oxford, U. K.
- D'Souza, R. M., N. H. Margolus, and M. A. Smith (2002), Dimension-splitting for simplifying diffusion in lattice-gas models, *J. Stat. Phys.*, *107*, 401–421.
- Flekkøy, E. G. (1993), Lattice Bhatnagar-Gross-Krook models for miscible fluids, *Phys. Rev. E*, *47*, 4247–4257.
- Fourar, M., S. Bories, R. Lenormand, and P. Persoff (1993), Two-phase flow in smooth and rough fractures, *Water Resour. Res.*, *29*(11), 3699–3708.
- Freidman, S. P. (1999), Dynamic contact angle explanation of flow rate-dependent saturation-pressure relationships during transient liquid flow in unsaturated porous media, *J. Adhesion Sci. Technol.*, *13*, 1495–1518.
- Glauz, R. D., and D. E. Rolston (1989), Optimal design of two-chamber, gas diffusion cells, *Soil Sci. Soc. Am. J.*, *53*, 1619–1624.
- Jones, S. B., and D. Or (1999), Microgravity effects on water flow and distribution in unsaturated porous media: Analyses of flight experiments, *Water Resour. Res.*, *35*, 929–942.
- Jones, S. B., D. Or, and G. E. Bingham (2003), Gas diffusion measurement and modeling in coarse-textured porous media, *Vadose Zone J.*, *2*, 602–610.
- Keshock, E. G., C. S. Lin, M. E. Harrison, L. G. Edwards, J. Knapp, and X. Zhang (1998), Measurement of two-phase flow characteristics under microgravity conditions, paper presented at Fourth Microgravity Fluid Physics and Transport Phenomena Conference, Natl. Cent. for Microgravity Res. on Fluids and Combust., Cleveland, Ohio.
- Marshall, T. J. (1959), The diffusion of gases through porous media, *J. Soil Sci.*, *10*, 79–82.
- Merks, R. M. H., A. G. Hoekstra, and P. M. A. Slood (2003), The moment propagation method for advection-diffusion in the lattice Boltzmann method: Validation and Peclet number limits, *J. Comput. Phys.*, *183*, 563–576.
- Millington, R. J. (1959), Gas diffusion in porous media, *Science*, *130*, 100–102.
- Millington, R. J., and J. M. Quirk (1961), Permeability of porous solids, *Trans. Faraday Soc.*, *57*, 1200–1207.
- Millington, R. J., and R. C. Shearer (1971), Diffusion in aggregated porous media, *Soil Sci.*, *111*, 372–378.
- Moldrup, P., T. Olesen, J. Gamst, P. Schjonning, T. Yamaguchi, and D. E. Rolston (2000), Predicting the gas diffusion coefficient in repacked soil: Water-induced linear reduction model, *Soil Sci. Soc. Am. J.*, *64*, 1588–1594.
- Nourgaliev, R. R., T. N. Dinh, T. G. Theofanous, and D. Joseph (2003), The lattice Boltzmann equation method: Theoretical interpretation, numerics and implications, *Int. Multiphase Flow, J.*, *29*, 117–169.
- Persoff, P., and K. Pruess (1995), Two-phase flow visualization and relative permeability measurement in natural rough-walled rock fractures, *Water Resour. Res.*, *31*, 1175–1186.
- Podolsky, I., and A. Mashinsky (1994), Peculiarities of moisture transfer in capillary-porous soil substitutes during space flight, *Adv. Space Res.*, *14*(11), 39–46.
- Prazak, J., M. Sir, F. Kubik, J. Tywoniak, and C. Zarcone (1992), Oscillation phenomena in gravity-driven drainage in coarse porous-media, *Water Resour. Res.*, *28*(7), 1849–1855.
- Schramm, L. L., D. Hart, F. Wassmuth, J. C. Legros, E. N. Stasiuk, and N. N. Smirnov (2003), Capillary flow in porous media under highly reduced gravity investigated through high altitude parabolic aircraft flights and NASA space shuttle flight, paper presented at Canadian International Petroleum Conference, Pet. Soc., Calgary, Alberta, Canada.
- Shan, X., and H. Chen (1994), Simulation of non-ideal gases and liquid-gas phase transitions by the lattice Boltzmann equation, *Phys. Rev. E*, *49*, 2941–2948.
- Shan, X., and G. Doolen (1996), Diffusion in a multicomponent lattice Boltzmann equation model, *Phys. Rev. E*, *54*, 3614–3620.
- Steinberg, S., J. I. D. Alexander, N. E. Daidzic, S. Jones, G. Kluitenberg, D. Or, L. Reddi, and M. Tuller (2003) Flow and distribution of fluid phases through porous plant growth media in microgravity, paper presented at Bioastronautics Investigator's Workshop, NASA, Galveston, Tex., 13–15 Jan.
- Succi, S. (2001), *The Lattice Boltzmann Equation for Fluid Dynamics and Beyond*, Clarendon, Oxford, U. K.

- Sukop, M. C., and D. Or (2003), Invasion percolation of single component, multiphase fluids with lattice Boltzmann models, *Physica B*, 338, 298–303.
- Sukop, M. C., and D. Or (2004), Lattice Boltzmann method for modeling liquid-vapor interface configurations in porous media, *Water Resour. Res.*, 40, W01509, doi:10.1029/2003WR002333.
- Welty, J. R., C. E. Wicks, R. E. Wilson, and G. L. Rorrer (2001), *Fundamentals of Momentum, Heat, and Mass Transfer*, 4th ed., John Wiley, Hoboken, N. J.
- Yendler, B. S., B. Webbon, I. Podolski, and R. J. Bula (1996), Capillary movement of liquid in granular beds in microgravity, *Adv. Space Res.*, 18(4/5), 233–237.
- Yoshino, M., and T. Inamuro (2003), Lattice Boltzmann simulations for flow and heat/mass transfer problems in a three-dimensional porous structure, *Int. J. Numer. Methods Fluids*, 43, 183–198.
-
- J. F. Chau and D. Or, Department of Civil and Environmental Engineering, University of Connecticut, 261 Gleenbrook Road, Unit 2037, Storrs, CT 06269, USA. (chau@engr.uconn.edu; dani@engr.uconn.edu)
- M. C. Sukop, Department of Earth Sciences, Florida International University, Miami, FL 33199, USA. (sukopm@fiu.edu)